

doi: 10.15407/ujpe62.08.0699

H.S. RASHEED,<sup>1,2</sup> NASER M. AHMED,<sup>1</sup> M.Z. MATJAFRI<sup>1</sup><sup>1</sup> Institute of Nano-Optoelectronics Research and Technology Laboratory (INOR),  
Universiti Sains Malaysia, School of Physics  
(Penang, Malaysia)<sup>2</sup> Department of Physics, College Of Education, Al-Mustansiriya University  
(Baghdad, Iraq)**NEW ZnO/Au/ZnO MULTILAYER FIELD  
EFFECT TRANSISTOR WITH EXTENDED  
GATE AS A SENSING MEMBRANE**PACS 73.61.Cw, 78.66.Db,  
82.47.Rs

ZnO/Au/ZnO (ZAuZ) multilayer structures with different thicknesses are deposited on a glass substrate by using the RF and DC magnetron sputtering methods and then are used as extended gates in field effect transistors (FET) for the pH detection. Their structural, optical, and electrical properties are investigated. The thickness parameter affected the pH sensitivity of the multilayers, by increasing the sensitivity from  $0.25 \mu\text{A}^{1/2}/\text{pH}$  to  $0.3 \mu\text{A}^{1/2}/\text{pH}$  in the saturation region and from  $50 \text{ mV}/\text{pH}$  to  $66.66 \text{ mV}/\text{pH}$  in the linear region. On the contrary, in the hysteresis voltage case, it is reduced from  $10.11 \text{ mV}$  to  $9.87 \text{ mV}$ , as the thickness of multilayers increases from (100/50/100) nm to (200/100/200) nm.

*Keywords:* EGFET, ZnO, hysteresis, multilayers, MOSFET.

**1. Introduction**

Recently, it was found that the metal-oxide-semiconductor field effect transistor (MOSFET) as one of the family of devices involving a field effect transistor and derived from an ion-sensitive field effect transistor (ISFET) (see, e.g., [1]) is of interest in the detection of ions and plays an important role in biosensor applications as a pH sensor. The extended gate field effect transistor (EGFET) was used to develop ISFET except for that the gate in the former was out and presented for first time by van der Spiegel in 1980 (see, e.g., [2]).

In studies of sensing materials such as ZnO, H.-H. Li *et al.* [3] achieved a higher sensitivity of ZnO/Si nanowires as EGFET for a pH sensitivity of  $0.73 \mu\text{A}^{1/2}/\text{pH}$  in the range of pH  $1 \rightarrow 13$  of buffer solutions.

A. Shenoy *et al.* [4] prepared ZnO nanowires by the spray pyrolysis method and tested as EGFET. In the pH sensor applications, the sensitivity of films was  $158.605 \mu\text{A}^{1/2}/\text{pH}$ .

In this paper, we produce ZnO/Au/ZnO multilayers with different thicknesses and use them as an ex-

tended gate in FET, by applying as pH sensors. The effect of the thickness parameter on the sensitivity of multilayers is investigated.

**2. Methodology****2.1. Growth of ZnO/Au/ZnO  
multilayer films**

Glass substrates (1 cm  $\times$  3 cm) in size were used to deposit ZnO/Au/ZnO multilayer thin films. The glass slide was ultrasonically cleaned in acetone and deionized water and then dried with nitrogen. The deposition of ZnO/Au/ZnO multilayers consists of three steps. First, a *n*-type ZnO layer was sputtered on the glass substrate; second, an Au metal layer was deposited on the ZnO layer; and, finally, a ZnO layer was deposited on the Au layer. So, three layers ZnO/Au/ZnO were formed, by using an HHV Auto 500 vacuum coater with a turbo molecular pumping system and RF and DC magnetron sputtering systems. The base pressure was  $4.35 \times 10^{-5}$  mbar, and the pressures during the working were  $6.75 \times 10^{-3}$  mbar for a ZnO target and  $5.6 \times 10^{-3}$  mbar for an Au target. The RF and DC were fixed at 100 W. All multilayers were fabricated with the use of ZnO targets (99.999% purity) and Au targets

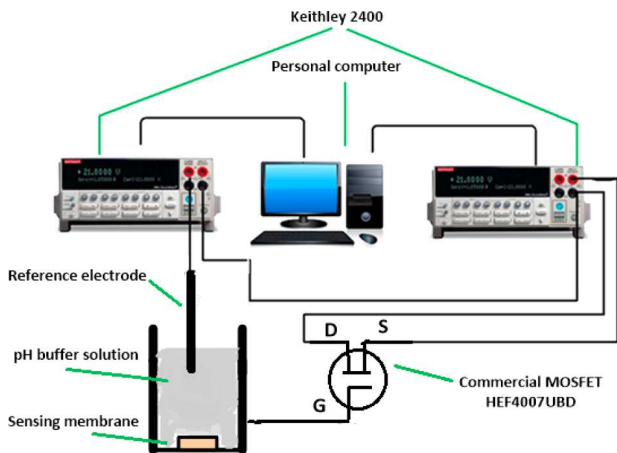


Fig. 1. pH sensor set up

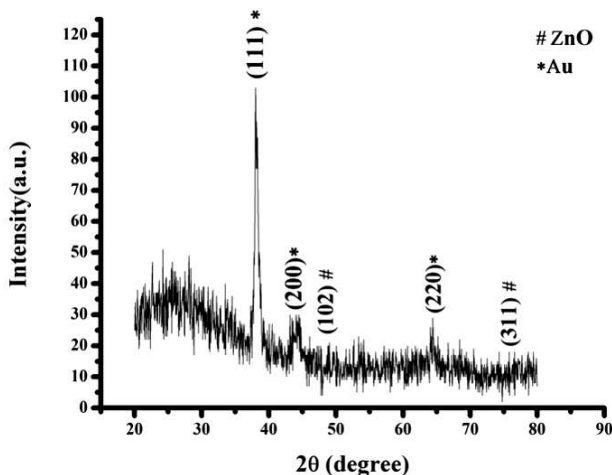


Fig. 2. ZAuZ XRD pattern

(99.999% purity). The thicknesses of ZnO/Au/ZnO multilayers were controlled by the sputtering time and set to be (200/100/200) nm and (100/50/100) nm.

### 2.2. Characterization of ZnO/Au/ZnO multilayer films

The equipment used to investigate the structural, optical, and electrical properties of the multilayer films after the deposition was an X-ray diffractometer equipped with a CuK $\alpha$  source ( $\lambda = 0.15418$  nm) to check the intensity peak and the crystallinity structure of ZnO/Au/ZnO multilayer films. For the nanoscale analysis, the atomic force microscopy (AFM) was used to determine the morphology and

roughness of the multilayer film by 3D images. We applied a field emission scanning electron microscope FEI NOVA Nano SSM450 to examine the top view of ZnO/Au/ZnO multilayers for various thicknesses and, finally, measured the resistivity and Hall mobility of the multilayer structures, by using the Hall effect, on an HL 5500 pc-hall effect device (Accent optical technologies Inc.).

### 2.3. Measurement of the performance of ZAuZ multilayers. EGFET as a pH sensor

The system seen in the schematic below was used in measurements of the electrical properties of ZnO/Au/ZnO multilayers as an extended gate field effect transistor. The electrical circuit includes two Keithley 2400 instruments, personal computer (PC) to store data and to analyze, commercial MOSFET HEF4007UBD (its drain and source being connected to one of the Keithley instruments), and the gate of MOSFET connected to the sensing membrane (ZnO/Au/ZnO), which was immersed in a pH buffer solution put in a cavity, reference electrode to calculate the sensitivity and hysteresis of the sensing membrane, and a pH buffer solution in the range (4  $\rightarrow$  10).

## 3. Results and Discussion

### 3.1. Properties of multilayer structures

When the growth of ZAuZ multilayers was completed, the phases and peaks of multilayer films were investigated by the X-ray diffraction analysis.

In Fig. 2, we show the XRD results, which indicate that the ZnO/Au/ZnO multilayers of different thicknesses have the same phase and that the polycrystallinity of films with intense Au peaks (111), (200), (220) has a cubic structure with lattice constants  $a = b = c = 4.0796$ , Å, while ZnO has hexagonal structure with the intense peaks (102) and (311) and the lattice constants  $a = b = 3.2648$  Å,  $c = 5.2194$  Å. From the results above, it is seen that the thickness has no effect on XRD results contrary to AFM results. The AFM analysis of 3D images indicates that the average roughness ( $R_a$ ) increases from 0.5 nm to 1 nm with the thickness of multilayers from 100/50/100 nm to 200/100/200 nm.

The  $R_a$  data show the irregularities in the surface of multilayers represented by projections and valleys (see Fig. 3, (a, b)).

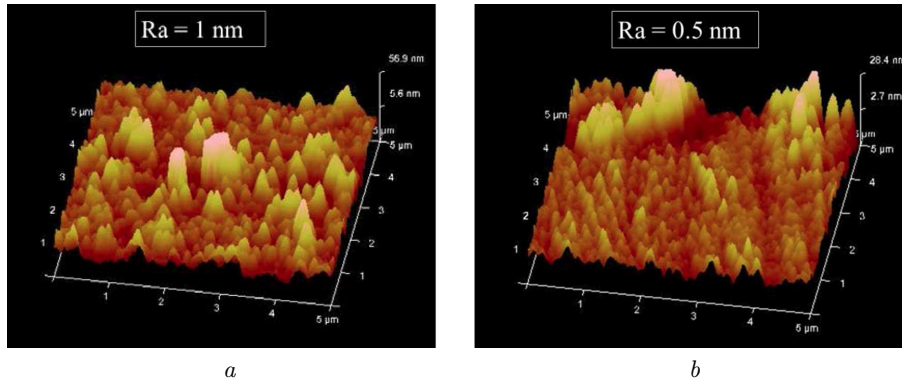


Fig. 3. AFM analysis of ZnO/Au/ZnO multilayers: 200/100/200 nm(a); 100/50/100 nm (b)

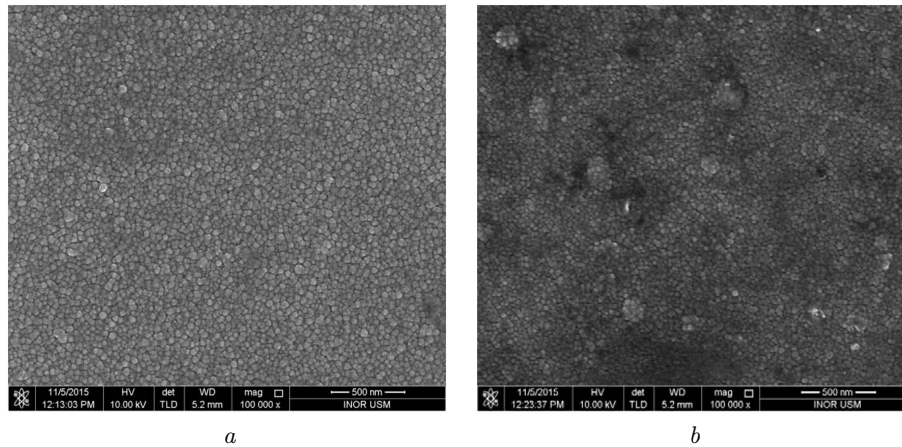


Fig. 4. ZnO/Au/ZnO multilayer FESEM images: 200/100/200 nm (a); 100/50/100 nm (b)

From FESEM images (Fig. 4, a, b), we can see a quite homogeneous surface of the films due to the RF and DC sputtering methods used to deposit the multilayer films.

### 3.2. Electrical properties of ZnO/Au/ZnO multilayers

The sheet resistance, Hall mobility, and Q-factor were calculated for ZnO/Au/ZnO with thicknesses of 200/100/200 and 100/50/100 nm. From the results presented in Table 1, we see that the sheet resistance of ZnO/Au/ZnO decreases, as the thickness of multilayers increases. This is attributed to that the resistivity of multilayers obeys the Ohm law according to the relation

$$\frac{1}{R_{\text{Total}}} = \frac{2}{R_{\text{ZnO}}} + \frac{1}{R_{\text{Au}}} \cong \frac{1}{R_{\text{Au}}}, \quad (1)$$

where  $R_{\text{Total}}$  is the total resistivity of multilayers,  $R_{\text{ZnO}}$  the resistivity of a ZnO layer, and  $R_{\text{Au}}$  the resistivity of the Au layer.

On the contrary, the results on the Hall mobility show that its value increases with decrease in the thickness of the multilayers (ZnO).

#### Electrical properties of ZnO/Au/ZnO at different thicknesses of multilayers

Film structure	Sheet resistance ( $\Omega/\square$ )	Hall mobility ( $\text{cm}^2/\text{Vs}$ )	Q-factor $\Phi_{Tc} = T^{10}/R_{\text{sh}}(\Omega^{-1})$
ZnO/Au/ZnO 200/100/200 nm	12.72	121.39	$4.019 \times 10^{-3}$
ZnO/Au/ZnO 100/50/100 nm	22.31	103.55	$3.467 \times 10^{-4}$

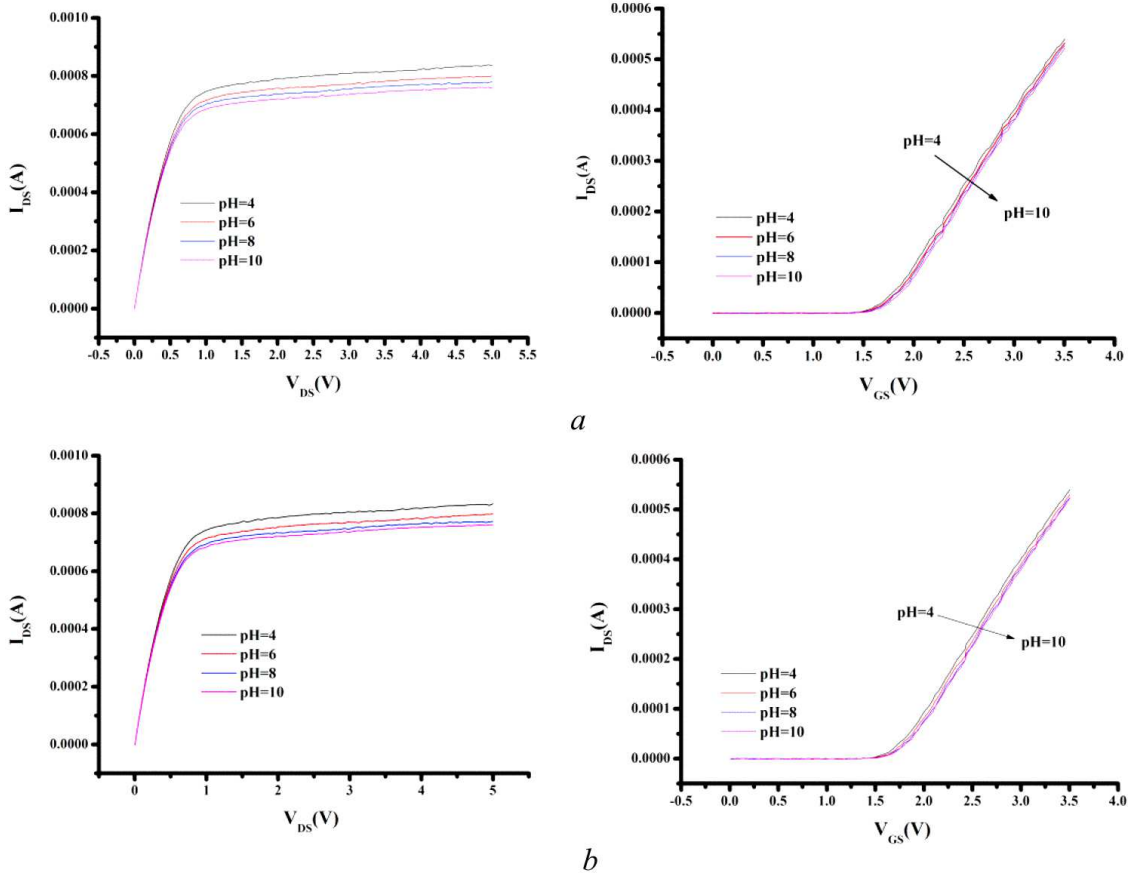


Fig. 5.  $I$ - $V$  characteristic curves for ZnO/Au/ZnO multilayers in the saturation region (a) and the linear region (b)

The Q-factor for ZnO/Au/ZnO multilayers that plays an important role in measurements of the performance of the multilayer device is calculated, by using the Hank relation [see also (4)]

$$\mathcal{Q}_{TC} = \frac{T^{10}}{R_{sh}}, \quad (2)$$

where  $\mathcal{Q}_{TC}$  is the Hank Q-factor,  $T$  the average optical transmission of the multilayers, and  $R_{sh}$  the sheet resistance of the multilayers.

### 3.3. pH-sensing membrane

The drain source current versus the drain source voltage ( $I_{DS}$ - $V_{DS}$ ) and the drain source current versus the gate source voltage ( $I_{DS}$ - $V_{GS}$ ) for the multilayers of ZnO/AD/ZnO for thicknesses of (200/100/ 200) and (100/50/100) nm are presented in Fig. 5, (a, b). On the left side called the saturation region,  $I_{DS}$

decreases with increase in the pH value, which is attributed to the accumulation of  $H^+$  in an acidic solution, while the right side of Fig. 5 shows the linear region, where  $I_{DS}$  increases with pH.

To calculate the performance of a sensing membrane represented by the chemical sensitivity, we use the site binding model [5] with the surface potential depending on pH, as expressed by the relation

$$2.303(\text{pH}_{pzc}-\text{pH}) = \frac{q\varphi}{kT} + \sinh^{-1} \frac{q\varphi}{kT\beta}, \quad (3)$$

where  $\text{pH}_{pzc}$  is the pH value at the point with zero charge,  $K$  Boltzmann constant, and  $T$  the absolute temperature.

The chemical sensitivity  $\beta$  depends on the number of surface sites per unit area  $N_s$ :

$$\beta = \frac{2N_s q^2 (k_b/k_a)^{1/2}}{KTC_{DL}}, \quad (4)$$

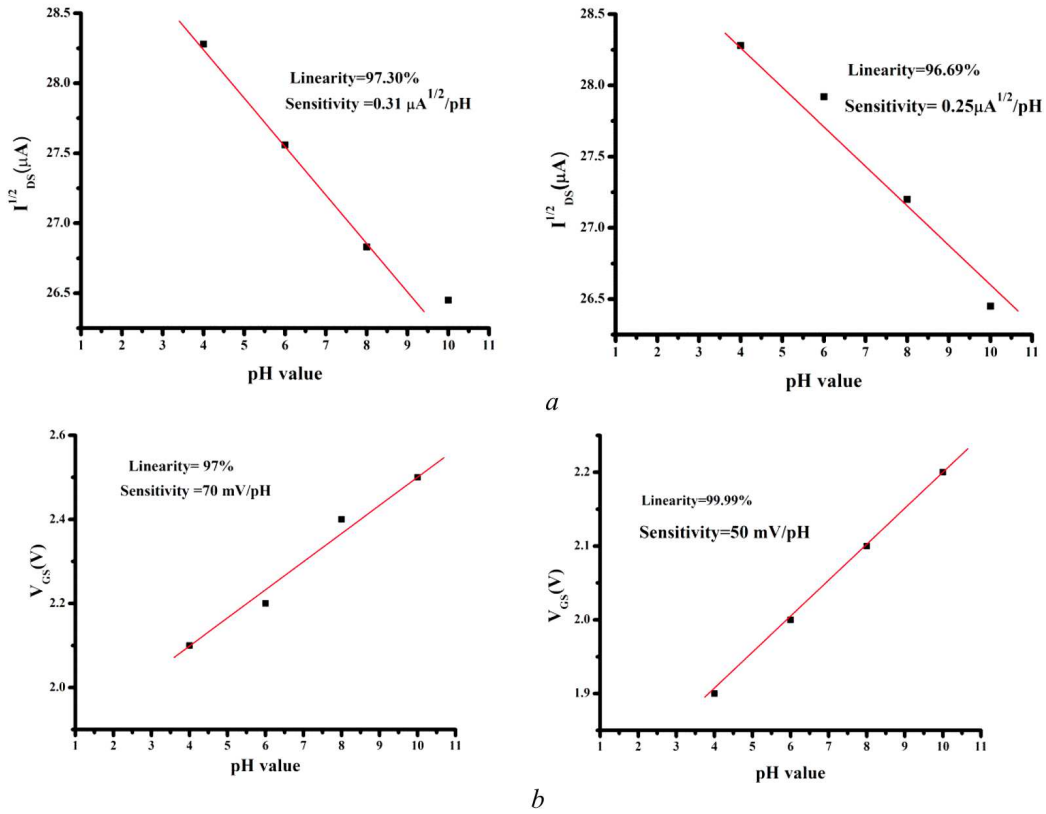


Fig. 6. The sensitivity plot of the ZnO/Au/ZnO multilayers in the saturation region (a) and in the linear region (b)

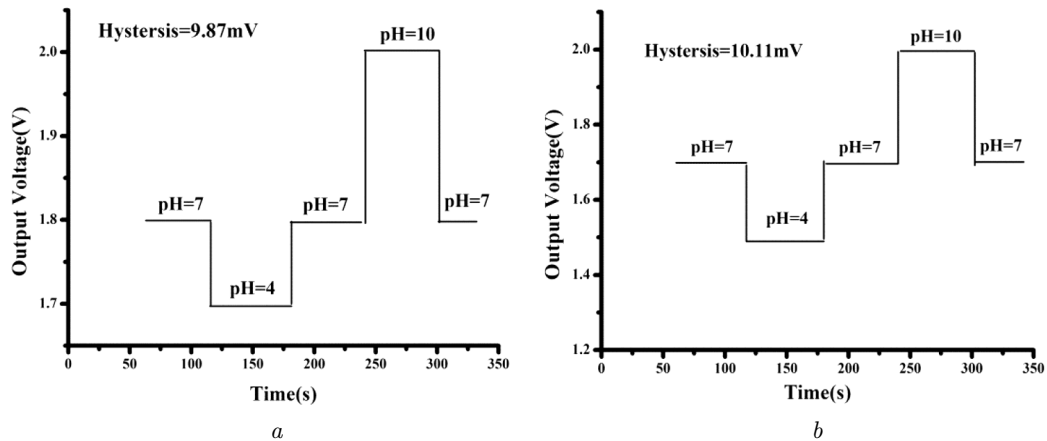


Fig. 7. Hysteresis of the (ZAuZ) multilayers at different thicknesses: (200/100/200) nm (a) and (100/50/100) nm (b)

where  $K_a$  and  $K_b$  are constants, and  $C_{DL}$  is the electric capacitance. From relation (2), higher  $N_S$  lead to higher  $\beta$ .

The left and right sides of Fig. 7, a show the saturation sensitivity of ZnO/Au/ZnO for thicknesses of (200/100/200) nm and (100/50/100) nm, respective-

ly. The sensitivity was calculated by plotting the square root of  $I_{DS}$  in  $\mu A$  versus pH [6]:

$$\text{pH sensitivity (saturation region)} = \frac{\Delta\sqrt{I_{DS}}}{\Delta\text{pH}}. \quad (5)$$

The higher sensitivity equal to  $0.31 \mu A^{1/2}/\text{pH}$  is revealed by the multilayers with higher thicknesses of (200/100/200) nm. The linear sensitivity seen in the left side of Fig. 7, *b* for multilayers with thicknesses of (200/100/200) nm is higher than a sensitivity of 50 mV/pH for the multilayers with thicknesses of (100/50/100) nm. This implies that a higher thickness leads to a higher sensitivity, which is attributed to the higher surface-to-volume ratio. This result is in agreement with relation (4).

#### 4. Hysteresis Characteristic

The hysteresis phenomena are related to many chemical interactions between ions and the defects of the sensing membrane surface and can define the difference between the high loop  $7 \rightarrow 10 \rightarrow 7$  and low loop  $7 \rightarrow 4 \rightarrow 7$  hysteresis voltages of ZnO/Au/ZnO multilayers, which are different for thicknesses of (200/100/200) nm and (100/50/100) nm, as is seen in Fig. 7, *a*.

#### 5. Conclusion

In this research work, we have reported on the synthesis of multilayers ZnO/Au/ZnO with different thicknesses, by using the RF and DC magnetron sputtering methods. For the first time, we have produced the films as extended gate field effect transistors. The multilayers have single cystalinity with the intense Au peak (111) investigated by the XRD technique. The multilayer films with thicknesses of 200/100/200 nm have higher saturation and linear sensitivity ( $0.31 \mu A^{1/2}/\text{pH}$ , 70 mV/pH) as compared with the films with thicknesses of (100/50/100) nm ( $0.25 \mu A^{1/2}/\text{pH}$ , 50 mV/pH), on the contrary with the hysteresis case.

We gratefully acknowledge the support of the USM Research University (grant 1001/PFIZsK/811220) and the Malaysian Ministry of Higher Education (fundamental research grant 203/PFIZIK/6711349).

1. A. Das, D.H. Ko, C.-H. Chen, M.-B. Chang, C.-S. Lai, F.-C. Chu, L. Chow, R.-M. Lin. Highly sensitive palladium oxide thin film extended gate FETs as pH sensor. *Sensors and Actuators B: Chem.* **205**, 199 (2014).
2. J. Qi, H. Zhang, Z. Ji, M. Xu, Y. Zhang. ZnO nano-array-based EGFET biosensor for glucose detection. *Appl. Phys. A* **119**, 807 (2015).
3. H.-H. Li, C.-E. Yang, C.-C. Kei, C.-Y. Su, W.-S. Dai, J.-K. Tseng, P.-Y. Yang, J.-C. Chou, H.-C. Cheng. Coaxial-structured ZnO/silicon nanowires extended-gate field-effect transistor as pH sensor. *Thin Solid Films* **529**, 173 (2013).
4. A. Shenoy *et al.* Sensing performance of EGFET pH sensors with zinc oxide (ZnO) nanowires. *Inter. J. Nanosci. Nanotechnol.* **1**, 85 (2015).
5. J.Y. Li, S.P. Chang, S.J. Chang, T.Y. Tsai. Sensitivity of EGFET pH sensors with TiO<sub>2</sub> nanowires. *ECS Solid State Lett.* **3**, 123 (2014).
6. N.H. Al-Hardan, M.A.A. Hamid, N.M. Ahmed, A. Jalar, R. Shamsudin, O.U. Othman, L.K. Keng, W. Chik, H.N. Al-Rawi. High sensitivity pH sensor based on porous silicon (PSi) extended gate field-effect transistor. *Sensors* **16**, 839 (2016).

Received 17.05.17

*X.C. Рашид, Н.М. Ахмед, М.З. Матджафрі*

НОВИЙ ZnO/Au/ZnO ПОЛЬОВИЙ  
ТРАНЗИСТОР З ШИРОКИМ ЗАТВОРОМ  
ЯК СЕНСОРНА МЕМБРАНА

Резюме

ZnO/Au/ZnO (ZAuZ) багатонашарові структури різної товщини утворені РЧ і ПТ-магнетронним розпиленням і потім використані як широкий затвор у польовому транзисторі для вимірювання рН. Досліджено їх структуру, оптичні та електричні властивості. Товщина структур впливає на рН-чутливість, яка росте від  $0,25 \mu A^{1/2}/\text{pH}$  до  $0,3 \mu A^{1/2}/\text{pH}$  в області насичення і від 50 мВ/рН до 66,66 мВ/рН на лінійній ділянці на відміну від випадку з гістерезисом, коли чутливість зменшується від 10,11 мВ до 9,87 мВ, якщо товщина зростає від (100/50/100) нм до (200/100/200) нм.